Bioorthogonal Chemistry Hot Paper

How to cite: *Angew. Chem. Int. Ed.* **2021**, *60*, 22017–22025
International Edition: doi.org/10.1002/anie.202108899
German Edition: doi.org/10.1002/ange.202108899

Exporting Metal-Carbene Chemistry to Live Mammalian Cells: Copper-Catalyzed Intracellular Synthesis of Quinoxalines Enabled by N–H Carbene Insertions

Sara Gutiérrez, María Tomás-Gamasa, and José L. Mascareñas**

Abstract: *Implementing catalytic organometallic transformations in living settings can offer unprecedented opportunities in chemical biology and medicine. Unfortunately, the number of biocompatible reactions so far discovered is very limited, and essentially restricted to uncaging processes. Here, we demonstrate the viability of performing metal carbene transfer reactions in live mammalian cells. In particular, we show that copper (II) catalysts can promote the intracellular annulation of alpha-keto diazocarbenes with ortho-amino arylamines, in a process that is initiated by an N-H carbene insertion. The potential of this transformation is underscored by the in cellulo synthesis of a product that alters mitochondrial functions, and by demonstrating cell selective biological responses using targeted copper catalysts. Considering the wide reactivity spectrum of metal carbenes, this work opens the door to significantly expanding the repertoire of life-compatible abiotic reactions.*

Introduction

Live cells can be viewed as microfactories that perform thousands of simultaneous chemical reactions in a highly regulated manner. Most of these reactions are promoted by enzymes, proteins that have evolved to exhibit exquisite rates and selectivities.[1] Over one-third of the enzymes feature metals at their active sites, and therefore are coined as metalloenzymes. In recent years, there has been an impressive progress in the creation of laboratory versions of metalloenzymes that catalyze "new-to-nature" reactions.[2] However, the application of these catalytic metalloproteins has been essentially restricted to the realm of synthetic methodology.[3] Their use for regulating and modifying biological behaviors, working under the same environment of native enzymes (living cells or organisms), remains to be uncovered.

An alternative approach to perform artificial chemical reactions in live cells has recently emerged, and consists of the use of exogenous, discrete transition metal catalysts.[4] While the catalytic activity of these reagents is far away from that of metalloenzymes, they can permeate living cells, and eventually trigger non-native organometallic reactions. Therefore, several transition-metal reagents that mediate intracellular allylic or propargylic deprotections,[5] cyclizations,[6] cross couplings,[7] or even formal cycloadditions,[8] have been recently disclosed.

However, the portfolio of reactions is yet too small, especially when compared with the enormous breadth and potential that organometallic catalysts exhibit in organic solvents. A particularly powerful class of catalytic organometallic reagents that have never been explored in mammalian cell environments, are discrete metal carbenes.[9] This might be in part due to the notion that these intermediates, and even their diazo precursors, are too fragile and reactive, and might not survive in water, and especially in the presence of native biomolecules with reactive nucleophilic functionalities like amines or thiols (Figure 1a, left). However, some isolated examples suggest that diazocompounds can be used for bioorthogonal tagging.[10] Moreover, several chemoselective functionalizations of peptides and proteins relying on C–H activations promoted by rhodium carbenes have been reported.[10d–e,11] Gillingham and co-workers have also described DNA modification reactions using rhodium or copper (I) carbenes capable of inserting into the N–H bond of adenines.[12]

In addition to these examples, metallocarbene transfer reactions have been developed in the context of artificial metalloenzymes, using heme-containing proteins expressed in *E. coli*, especially with native iron-containing cofactors;[13] though these advances can be ascribed to the fields of synthetic chemistry and synthetic biology.[14]

In this context, we questioned whether it would be possible to perform carbene transfer reactions with discrete transition metal catalysts in biorelevant aqueous mixtures, and especially in the complex environment of living mammalian cells (Figure 1). Adding this type of catalytic reactions to the catalog of life-compatible organometallic processes might foster new opportunities for cellular and biological intervention given the power and versatility of metal-carbene chemistry.

However, this goal raises many challenges and questions: Will diazo reagents be able to capture the metal complex in

[*] Dr. S. Gutiérrez, Dr. M. Tomás-Gamasa, Prof. J. L. Mascareñas
Centro Singular de Investigación en Química Biolóxica e Materiais Moleculares (CiQUS) and Departamento de Química Orgánica, Universidade de Santiago de Compostela
15705 Santiago de Compostela (Spain)
E-mail: maria.tomas@usc.es
joseluis.mascarenas@usc.es

Supporting information and the ORCID identification number(s) for the author(s) of this article can be found under: https://doi.org/10.1002/anie.202108899.

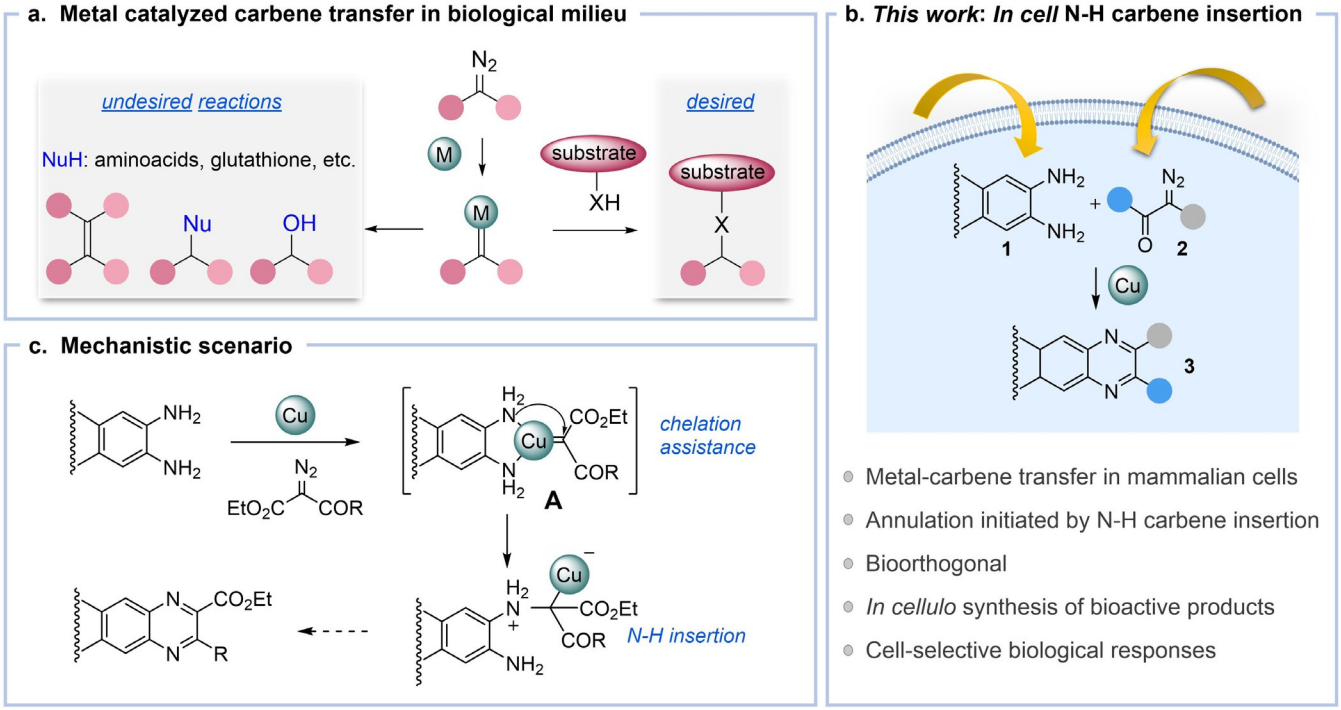

Figure 1. Metal N-H carbene insertions in biological settings. a) Orthogonality challenges in metal-mediated carbene transfer transformations in aqueous/biological media. b) Copper-promoted annulation initiated by an N-H carbene insertion within biological and/or cellular environments. c) Mechanistic outline: The bidentate coordination may allow the chelation of copper. This might favor the N-H insertion, which is followed by an intramolecular condensation and oxidative aromatization.

a challenging biological milieu to generate the metal carbenes? Are these metal-carbene intermediates compatible with biological molecules and stable enough to react with designed reactants? Can we perform this chemistry within living cells? Can we use these reactions to build abiotic bioactive products in cells, and elicit biological effects?

Herein we report the first metal-catalyzed carbene transfer reaction carried out in living mammalian cells. The reaction has been implemented with *ortho*-amino arylamines, providing for the assembly of photophysically and/or biologically relevant quinoxaline products (Figure 1b). The transformation likely benefits from a chelation assistance process to generate intermediates like **A**, which favor the N-H insertion, initial step of the process (Figure 1c). We also demonstrate that this technology can be used for the *in cellulo* synthesis of a compound that promotes mitochondrial fragmentation and depolarization, and produces cytotoxic effects. Importantly, by equipping the copper ligand with suitable targeting units, it is possible to elicit cell selective responses.

Results and Discussion

Finding the Right Catalyst. At the outset, we needed to identify a suitable reaction involving a metal-carbene transfer process that could be easily monitored, eventually, by fluorescence microscopy. In this context, we were attracted by the annulation between 1,2-diaminobenzenes and α-diazo-β-keto esters reported by Pandit and co-workers, which was described to work in water using different transition metal catalysts, and involves as initial step an N-H insertion of the metal carbene.[15] In particular, we selected as reactant diaminonaphthalene (**1**), which can provide fluorescent benzoquinoxalines such as **3a** (Figure 2a). We reasoned that the second amine group in the substrate could play an important role not only to drive the generation of cyclic products, but also as metal coordination handle to enhance reactivity and favor orthogonality in the presence of competing nucleophiles (Figure 1c).[16]

Our initial assays, consisting of the treatment of diamine **1** with 1 equiv of diazocarbonyl **2a** and 10 mol% of $Fe(OTf)_3$ in water (100 mM), at 40 °C for 24 h, led to no conversion.[15] Other iron (III) catalysts ($FeCl_3$, $Fe(acac)_3$) were also ineffective. However, using $Cu(OTf)_2$ as catalyst, **3a** was obtained in 56% yield (Figure 2a, entry 3). Further screening of copper salts allowed to identify $Cu(OAc)_2{\cdot}H_2O$ as a more efficient catalyst for this transformation, affording the product **3a** in 70% yield (entry 4; 55% after 3 h of reaction, using 10 mol% of the copper salt, Supporting Information, Table S3). The catalyst loading could be decreased to 5 mol% without affecting the yield. Even using 1 mol%, we observed more than 50% of the product (entry 5). It is important to note that the reaction mixtures consist of heterogeneous suspensions.

We also tested other transition metal complexes that had been previously used in carbene insertion reactions (Figure 2a and Table S1).[17] Using gold reagents like XPhos-$AuNTf_2$, we observed testimonial amounts of the desired adduct **3a** (14–18%, entry 6). Rhodium or iridium catalysts like $Rh_2(OAc)_4$, $[Rh(COD)Cl]_2$, $[Cp^*IrCl_2]_2$, $[Ir(COD)Cl]_2$

a. Metal screening and optimization

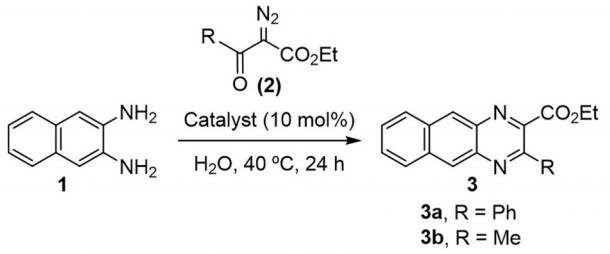

Entry	Catalyst	Yield **3a** [%][a]
1	-	0
2	$Fe(OTf)_3$	0
3	$Cu(OTf)_2$	56
4	$Cu(OAc)_2{\cdot}H_2O$	70
5[b]	$Cu(OAc)_2{\cdot}H_2O$	53
6	$XPhosAuNTf_2$	14
7	$[Ir(COD)Cl]_2$	49
8	$Rh_2(OAc)_4$	38
9	$Rh_2(esp)_2$	72
10[c]	$Rh_2(esp)_2$	50
11[d]	$Cu(OAc)_2{\cdot}H_2O$	93
12[e]	$Cu(OAc)_2{\cdot}H_2O$	67 (57[f], **3b**)
13	$[(MeCN)_4]CuPF_6$	62

b. Bioorthogonality

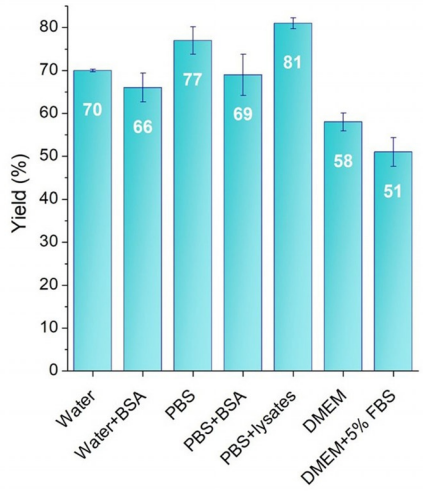

Figure 2. Metal-catalyzed assembly of quinoxalines. a) Metal-catalyzed assembly of quinoxalines in water. Metal screening and optimization. *Reaction conditions unless otherwise stated:* 1 equiv **1** and **2a**, in H_2O (100 mM), in presence of 10 mol% catalyst, and heating of the resulting heterogeneous mixture at 40 °C for 24 h. [a] Yield calculated by ^{1}H-NMR using 1,3,5-trimethoxybenzene as internal standard. [b] 1 mol% of the catalyst. [c] 5 mol% of the catalyst. [d] Substrate concentration: 5 mM. [e] **2b** was used as substrate. [f] Isolated yield; esp = α,α,α′,α′-tetramethyl-1,3-benzenedipropionic acid. b) Efficiency of the copper-carbene mediated synthesis of quinoxaline **3a** in presence of biological buffers. Reaction conditions: 1 equiv **1** and **2a** (substrates concentration: 100 mM), 10 mol% $Cu(OAc)_2$, 40 °C, 24 h; BSA 5 mg mL^{-1}; Cell lysates 4 mg mL^{-1} (the values are average of three experiments, and error bars are standard deviations).

and $[Ir(COD)(OMe)]_2$ did promote the reaction at 40 °C, but in modest yields (20–49%). With $Rh_2(esp)_2$, a more hydrophobic rhodium catalyst, the reaction was more efficient (72% yield, entry 9); however, using more diluted conditions, the reaction yield dropped to 50% (entry 10) and an undesired side product resulting from addition of water to the carbene was also formed in substantial amounts (**4**, $CO_2EtCH(OH)COPh$, 49%). Fortunately, this was not the case with $Cu(OAc)_2$, which led to good results under more diluted conditions (5 mM, entry 11).

Control experiments in the absence of diamine **1** led to a mixture of the diazo carbene dimer (**4′**) and the O-H insertion product **4** (Figure S1). Other diazo reagents could also be used, and therefore product **3b** was formed in a good 67% yield after 24 h (57% isolated yield, entry 12). The reaction can also be carried out with Cu^I salts, albeit with lower efficiency (entry 13, and Table S1). The use of cosolvents, such as acetonitrile or dimethylsulfoxide (10–20% v/v), allowed to carry out the reaction in a homogeneous solution, but didn't bring special improvements (Table S2). Even in the absence of solvent (neat conditions), **3a** was obtained in 59% yield.

Bioorthogonality. As the goal was moving to biological media, it was key to uncover the tolerance of the reaction to biological additives and salts (Figure 2b). Using 10 mol% of $Cu(OAc)_2{\cdot}H_2O$, and 100 mM of substrates, we were glad to observe that in saline phosphate buffer (PBS, pH 7.2) the reaction was even slightly more efficient than in water (77% after 24 h). Good results were also observed when the reaction was carried out in the presence of biological additives like BSA (bovine serum albumin, 5 mg mL^{-1}), a protein that features one free cysteine and several histidines in its structure. Importantly, the process is also compatible with the presence of HeLa cell lysates (protein content: 4 mg mL^{-1} in PBS, 81% yield after 24 h (Supporting Information, Section 4). Using lower catalyst loadings (5 mol%) the product was obtained in a satisfactory 73% yield, and at lower concentrations (25 mM) the yield decreased to 63% (SI, Table S4). Finally, the transformation is effective under more stringent conditions such as cell culture media like DMEM (Dulbecco's modified Eagle's medium), that contains many additives (vitamins, amino acids, etc.), although it is slightly less efficient (58% yield). Even in DMEM containing 5% of FBS (fetal bovine serum) the reaction takes place to give a 51% yield of the product.

The reaction works well in the presence of stoichiometric amounts of amino acids like lysine or tyrosine, or biomolecular additives such as glucose, guanine or cytosine (yields between 50–62%). It also tolerates amino acids like glutamic acid, histidine, cysteine or methionine, when used in equivalent amounts with respect to the copper catalyst. However, it is inhibited by additives like adenine or glutathione, very likely because these compounds coordinate to the copper catalyst producing inactive off-cycle complexes. Curiously, when the same reaction is performed in PBS instead of water, it tolerates the presence of glutathione (10 mol%), and the product was formed in a 66% yield (Table S5). This result suggests that saline media like PBS might accelerate the desired reaction owing to hydrophobic effects,[18] and perhaps

also disfavor the irreversible formation of inactive copper complexes.

Catalytic Reactivity in Mammalian Cells. The stage was set to move to a more complex scenario, such as that of living mammalian cells. Note that a cell medium cannot be fully equated to the above in vitro conditions, and might be better viewed as a heterogeneous, crowded gel. Fluorescence spectroscopy confirmed that whereas the diamine substrate **1** presents a very low emission above 500 nm when excited at 385 nm, the product **3a** displays high fluorescence (Figure S2,S3). These emission properties were also confirmed in living cells: incubation of HeLa cells with **3a** (100 μM), DMEM washing, and observation under the microscope, revealed a clear intracellular emission (Figure 3a, panel B), much higher that when adding **1** and **2a** (panel A). For the cellular reactions, HeLa cells were incubated with $Cu(OAc)_2$ for 50 min (50 μM) in DMEM, thoroughly washed to remove extracellular copper salts (2×DMEM) and thus minimize extracellular reactions, and treated with the substrates (**1** and **2a**, 100 μM each). Observation under the fluorescence microscope after 1.5 h revealed a clear intracellular buildup of green fluorescence in the cytosol, which must be associated to the formation of product **3a** (Figure 3a, panel C). Monitoring the process with time confirmed a progressive increase in total fluorescence intensity, in consonance with the generation of more product (Figure 3a, panel D and Figure S7). Control experiments of cells treated with the copper complex or with only one of the components, either **1** or diazo **2a**, led to essentially no fluorescence (Figure S8). Similar results were obtained using MCF7 cells (Figure 3a, panel E,F).

Morphological analysis of the cells after the reaction time was indicative of a reasonably good status in terms of viability. As the toxicity of copper salts could be an issue,[19] we performed specific cytotoxicity experiments in HeLa, MCF7 and HEK293 cell lines. As detailed in the Supporting Information (Section 10), using MTT assays we confirmed that the addition of the copper salt ($Cu(OAc)_2$, 50 μM) doesn't compromise the cell viability in any of the cell lines, even after 24 h. At higher concentrations (100 μM) we did observe some effect (62% cell viability after 24 h). Moreover, propidium iodide assays indicated that incubation of cells with 50 μM of copper salt for 6 h doesn't alter the cell membrane status in any of the cell lines. Furthermore, MTT studies showed that neither **1**, **2a** nor product **3a** affected the viability of the cells (complete survival after 18 h). Very importantly, the intracellular presence of product **3a** was further confirmed by mass spectrometry, after extraction of the cell contents with MeOH (Figure 3b). Indeed, using this protocol (SI, Section 14) we could even quantify the product (over 4 μM in total) which combined with the amount of intracellular copper calculated using ICP analysis allowed to estimate a TON around 7 (after an incubation time of 5 h, Figure 3b, average of three experiments, Supporting Information, Sections 13 and 14).

Eliciting Biological Effects. Developing *in cellulo* metal-promoted transformations, and specifically metal carbene transfer reactions, is itself relevant from a fundamental perspective. However, a major challenge in the area is the

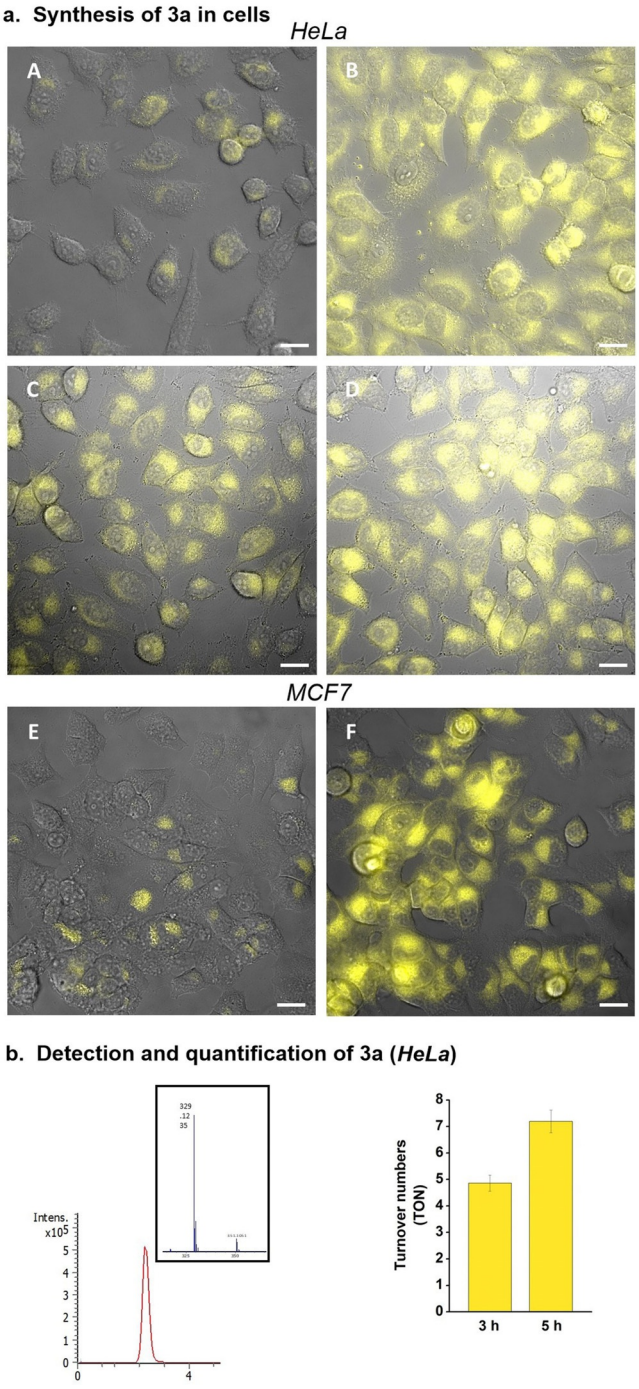

Figure 3. Synthesis of **3a** in cells. a) Fluorescence micrographies (brightfield) of HeLa (A–D) and MCF7 cells (E,F) after incubation with: **1** and **2a** (A,E); **3a** (B) or $Cu(OAc)_2$, washing, and treatment with **1** and **2a** for 1.5 h (C) or for 3 h (D,F). Reactions conditions: Cells were pretreated with 50 μM of $Cu(OAc)_2$ (stock solution in H_2O) for 50 min, washed twice with DMEM, and incubated with 100 μM of substrates **1** and **2a** (stock solutions in DMEM) for the indicated time. b) Detection and quantification of **3a** in HeLa cells. *Left*: Extracted ion chromatogram of the product (**3a**) generated intracellularly (methanolic extract), after 5 h of reaction; *Right*: Quantification of turnover numbers (average of three experiments), considering the product present in the cell media and washes (2×DMEM, 1×PBS) and in the methanolic (intracellular) extracts (which counts for over 75% of the total). Scale bar: 20 μm. $\lambda_{exc} = 385$ nm, $\lambda_{em} > 520$ nm. The residual fluorescence in A and E derives from **1** (see the SI, Figure S3).

demonstration that the reactions can find biological or biomedical applications. Indeed, several metal-promoted uncaging reactions have already been used to activate proteins or release bioactive agents in biological environments.[20] Conversely, "anabolic" processes, based on bond-forming reactions to build bioactive products, are much less developed.[21] Quinoxaline scaffolds are found in many biorelevant compounds, and therefore, we questioned whether our technology could enable the synthesis of bioactive derivatives inside live cells.

In this context, we were attracted by Tyrphostins (TYRosin PHOSphorylation INhibitors),[22] compounds that exhibit a variety of interesting biological profiles, apparently as a consequence of their tyrosine kinase inhibitory activity. Remarkably, whereas **3a** was rather innocuous to cells (Figure S6), benzoquinoxaline **3c**, also called Tyrphostin AG1385,[23] promoted a decrease in the cell viability of 40% after 12 h (50 μM). Noteworthy, using higher concentrations (100 μM) we didn't observe a further increase in the cell death (Figure 4b), a result that can be explained because of the tendency of this highly hydrophobic product to aggregate and precipitate, which compromises its internalization.[24] As expected, product **3c** can be readily made applying our carbene transfer methodology using reactants **1** and diazo compound **2c** (Figure 4a and Supporting Information, Section 6 for its in vitro synthesis).

Therefore, after addition of 50 μM of the reactants (**1** and **2c**) to HeLa cells previously treated with $Cu(OAc)_2$ (25 μM), we observed a similar effect in the cell viability than by direct incubation with 50 μM of **3c**. Significantly, in contrast to that observed with **3c**, using higher concentrations of the substrates (up to 100 μM) the effect on cell survival is higher (less than 30% of cell viability, Figure 4b). These results further highlight one of the potential advantages of generating bioactive products in situ versus their external addition.

Product **3c** presents low levels of fluorescence, which precludes its detection under the microscope; however, we could confirm and quantify its intracellular formation by MS of cellular extracts obtained after carrying out the reaction in cells (after 4.5 h we calculated TONs over 4, Supporting Information, Section 14). Given that some tyrphostins have been shown to affect mitochondria,[23] we tested whether the intracellular generation of **3c** could affect the mitochondrial membrane potential, a property that can be monitored by measuring the fading of TMRE (tetramethyl rhodamine methyl ester) staining.[25]

Gratifyingly, while treatment of HeLa cells with $Cu(OAc)_2$ and either substrate **1** or **2c** (100 μM) doesn't alter the mitochondria potential after 3.5 h (Figure 4c, panel A and Figure S9), addition of both reactants to cells previously treated with $Cu(OAc)_2$ (50 μM) led to a much more diffuse and less intense fluorescent signal of TMRE, indicating depolarized mitochondria, which is in consonance with the in situ formation of **3c** (Figure 4c, panel C). Indeed, direct addition of **3c** led to qualitatively similar results (Figure 4c, panel B).

The same effect was observed with other type of cancer cell lines like MCF7 (differences in staining in panels D–F) and HEK293 (Figure S10). Noticeably, leaving the HeLa cells for a longer time (8 h) allows to recover, at least partially, the TMRE staining, however the mitochondria presented a different morphology, consistent with a considerable fragmentation (Figure 4d, panels G,I,K and Figure S11). Using MitoTracker Green as mitochondrial dye, whose staining ability is less dependent on the polarization state of the organelles, we could confirm the fragmentation effect associated to the generation of **3c**. Cells treated only with substrates displayed a very well-defined network of tubular mitochondria, predominantly in fusion state (Figure 4d, panel H). However, addition of **3c** (100 μM) resulted in more fragmented mitochondria (Figure 4d, panel J). More importantly, a similar fragmented network, which is associated to fission, was also observed by generating the compound in situ, using our copper catalyzed transformation (Figure 4d, panel L and Figure S12).

Targeted Catalysts and Cellular Selectivity. A major dream in pharmacology is related to the possibility of delivering or accumulating drugs in specific, desired cellular targets. Even more attractive is the prospect of a catalytic generation of drugs in a cell-selective manner. We evaluated this possibility by building the conjugate **5**, shown in Figure 5a, which features an integrin-targeting motif (RGD: Arg-Gly-Asp) linked to a copper triazolyl ligand (BTTAA, Supporting Information, Section 7).[8c] Hypothetically, this tripeptide motif might favor the preferential targeting of cell lines expressing substantial amount of integrins, such as HeLa cancer cells.[26] The conjugate was also engineered to exhibit a rhodamine dye (TAMRA) linked to a lysine side chain, in order to monitor the cellular fate of the complex. The copper complex (**5-Cu**) was assembled in situ, just before the addition to cells, by treatment of hybrid **5** with $CuSO_4$ (0.5 equiv) in water (10 min). The formation of **5-Cu** was confirmed by LC-MS (Figure S5).

As depicted in Figure 5a (panel A), addition of **5-Cu** (15 μM) to HeLa cells, and subsequent washing (2xDMEM), gave rise to a substantial intracellular staining. In contrast, using MCF7 or HEK293 cells, which are known to exhibit lower levels of integrin receptors, we observed much less fluorescence (Figure 5a, panel B and Figure S13 for HEK293). Further analysis by CTCF (corrected total cell fluorescence) corroborated the better uptake of HeLa cells (Figure 5a, right). More importantly, in consonance with this programmed internalization of the copper complex, we observed a much higher increase in the fluorescence associated to the formation of product **3a** in the HeLa cells, after treatment with reactants **1** and **2a** (Figure 5b, panels C and D, respectively and Figure S14). It is important to note that using $Cu(OAc)_2$ instead of **5-Cu** as catalytic reagent MCF7 cells are able to generate the product (Figure 3), which confirms that the above cell selective responses are associated to the preferential targeting and internalization properties of our designed catalyst **5-Cu**.

This cell-dependent reactivity was also observed in the reaction leading to the mitochondria active quinoxaline **3c**. Therefore, treatment of the cells with **5-Cu** (15 μM), washings (2 × DMEM) and addition of **1** and **2c** (100 μM), led, after 3.5 h, to a substantial mitochondrial depolarization only in HeLa cells (Figure 5c, panel G). MCF7 and HEK293 cells

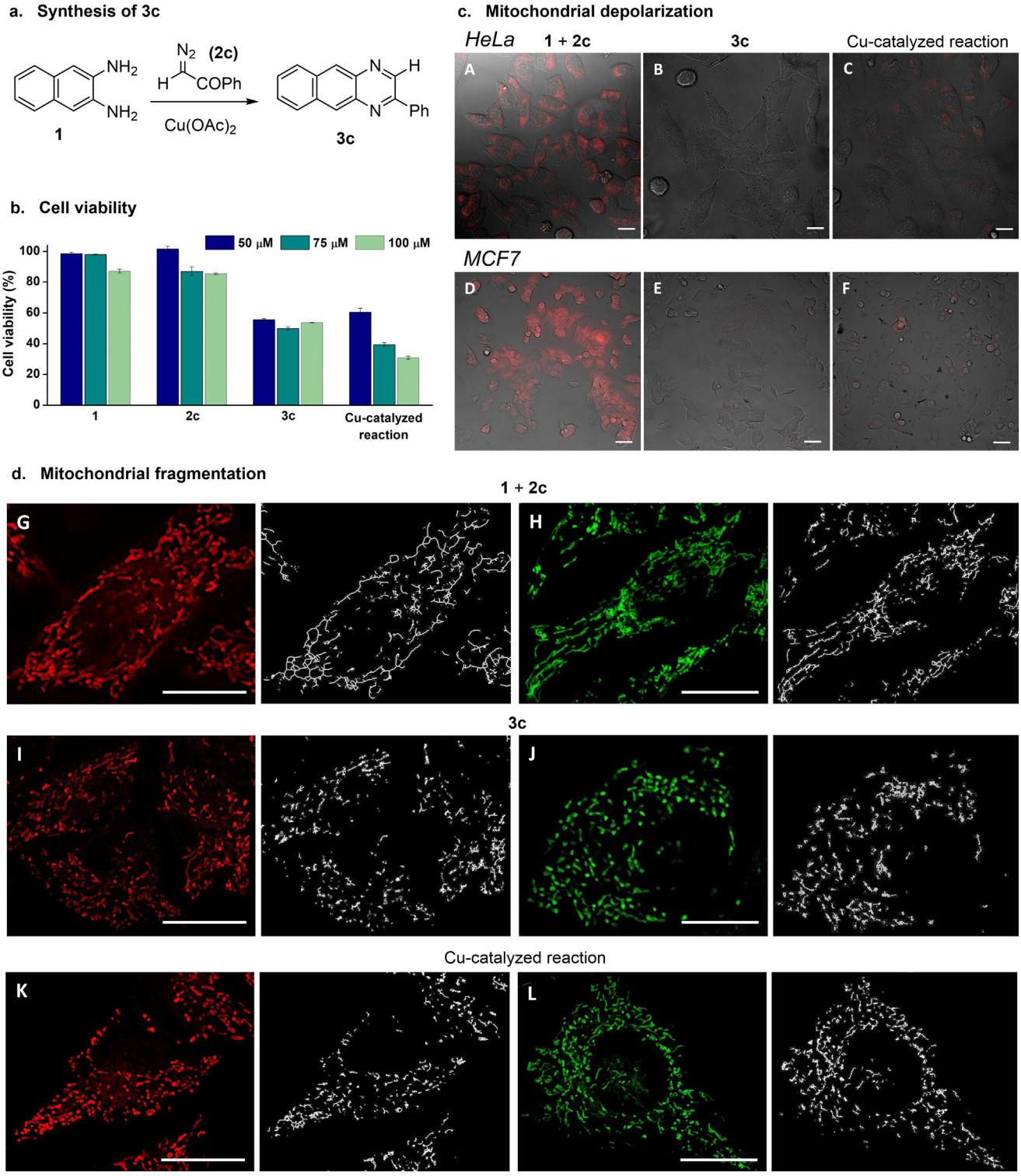

Figure 4. Generation of **3c** in cells. a) Synthesis of **3c**. b) Cytotoxicity studies. HeLa cells were mixed with either **1**, **2c**, or **3c** (50–100 μM) for 12 h; for the reaction, cells were incubated with $Cu(OAc)_2$ (25–50 μM) for 50 min, washed twice with DMEM and treated with substrates **1** and **2c** (50–100 μM) for 12 h. c) Mitochondrial depolarization. Fluorescence micrographies using TMRE as marker: HeLa (A–C), and MCF7 cells (D–F) (brightfield) after incubation with: **1** and **2c** (A,D); **3c** (B,E); $Cu(OAc)_2$, washing, and treatment with **1** and **2c** (C,F) for 3.5 h. d) Mitochondrial fragmentation. Fluorescence micrographies of HeLa cells (brightfield) using TMRE (G,I,K) or MitoTracker Green (H,J,L) as marker, after incubation with: **1** and **2c** (G,H); **3c** (I,J); or $Cu(OAc)_2$, washing and treatment with **1** and **2c** for 8 h (K) or 2 h (L); in white, mitochondrial staining from each image displayed as a skeleton network using the ImageJ skeleton filter, which allows a better visualization of the fragmentation. Reaction conditions: Cells were mixed with **1** and **2c**, or **3c**. For the reaction in cells, they were incubated with $Cu(OAc)_2$ (50 μM) for 50 min, washed twice with DMEM and treated with substrates **1** and **2c** (100 μM) and incubated with TMRE or MitoTracker Green (100 nM) for 10 min. Scale bar: 20 μm (15 μm in section c). $\lambda_{exc} = 550$ nm, $\lambda_{em} = 570–590$ nm for panels (A–G,I,K); $\lambda_{exc} = 470$ nm, $\lambda_{em} = 490–580$ nm for panels (H,J,L).

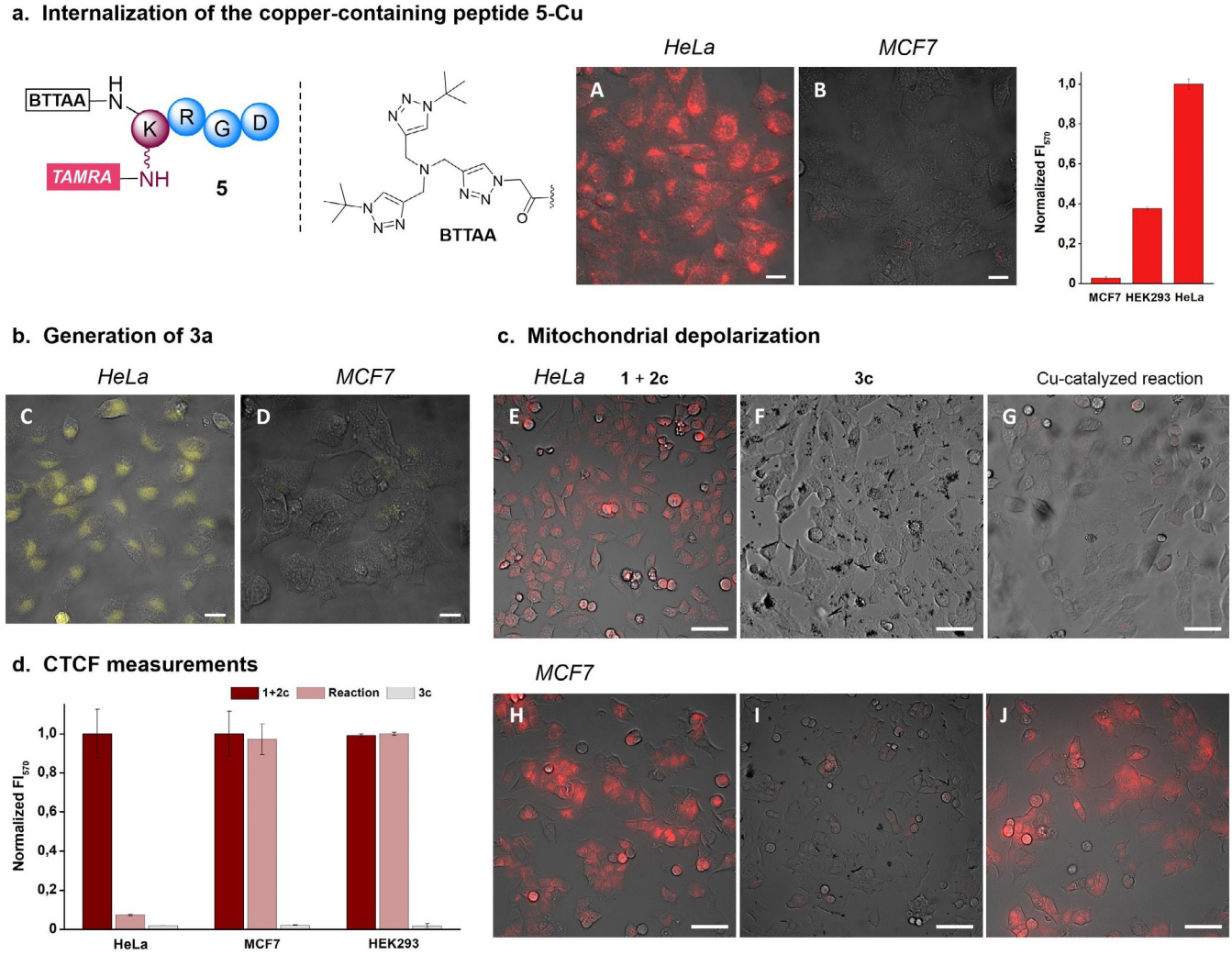

Figure 5. Selective cellular targeting using a RGD copper-containing peptide (**5-Cu**). a) Structure of the RGD containing ligand in **5-Cu**; Comparison of internalization of **5-Cu**. Fluorescence micrographies of HeLa (A) and MCF7 cells (B) (brightfield) and CTCF measurements in HeLa, MCF7 and HEK293 cells. Conditions: cells were incubated with 15 μM of **5-Cu** for 1.5 h. b) Fluorescence micrographies of HeLa (C) and MCF7 cells (D) (brightfield) after incubation with **5-Cu**, washing, and treatment with **1** and **2a** for 3.5 h. Scale bar: 20 μm. c) Cell-selective mitochondrial depolarization: Fluorescence micrographies of HeLa (E–G) and MCF7 cells (H–J) (brightfield) after incubation with: **1** and **2c** (E,H), product **3c** (F,I), or **5-Cu**, washing, and treatment with **1** and **2c** for 3.5 h (G,J). d) Bar graphic including CTCF measurements of mitochondrial depolarization in HeLa, MCF7 and HEK293 cells. Reaction conditions: cells were mixed with **5-Cu** (15 μM) for 1.5 h, washed twice with DMEM and treated with **1** and **2a**, or **1** and **2c** (100 μM) for 3.5 h followed by TMRE (100 nM) for 10 min. Scale bar: 100 μm. $\lambda_{exc} = 550$ nm, $\lambda_{em} = 570–590$ nm for panels (A,B,E-J); $\lambda_{exc} = 385$ nm, $\lambda_{em} > 520$ nm for panels (C,D).

remain essentially intact (Figure 5c, panel J and Figure S15). Control experiments with product **3c** revealed a similar depolarization effect in all cell lines, independently of their integrin expression (Figure 5b, panels F,I and Figure S15). Figure 5d represents a quantification of the resulting TMRE staining. MTT assays showed that **5-Cu** (20 μM) didn't compromise the cell viability of any of the cell lines, even after 18 h (SI, Figure S6).

All these results confirm the viability of using transition-metal carbene transfer catalysts for a cell selective synthesis of bioactive products and set the bases for future biological and biomedical applications.

Conclusion

We have described the first examples of a transition metal catalyzed carbene-transfer reaction occurring in living mammalian cells. The reaction entails a N-H insertion of a copper carbene into aromatic 1,2-diamines, and allows to generate benzoquinoxalines, owing to a subsequent intramolecular imine condensation and oxidative aromatization process. Therefore, the whole process, while capitalizing in the initial intermolecular carbene transfer reaction, involves two additional chemical steps. Preliminary studies confirmed the existence of a significative TON (of up to 7), which stresses the viability of performing intracellular catalytic carbene chemistry.

Importantly, we have also developed initial examples that underscore the biological potential of the approach. The catalytic chemistry can be used for the intracellular synthesis of mitochondrial fragmenting agents, providing for more efficient biological responses than when using a direct addition of the bioactive products. Moreover, by conjugating the copper catalyst to an integrin targeting moiety, it is possible to achieve cell-selective biological effects. The demonstration that metal-promoted reactions involving N-H carbene insertions can be carried out in the complex environment of a mammalian cell should foster further research to merge metal carbene catalysis and biological chemistry.

Acknowledgements

This work has received financial support from Spanish grants (PID2019-108624RB-I00, RTI2018-093813-J-I00 and ORFEO-CINQA network CTQ2016-81797-REDC), the Consellería de Cultura, Educación e Ordenación Universitaria (2015-CP082, ED431C-2017/19 and Centro Singular de Investigación de Galicia accreditation 2019–2022, ED431G 2019/03), the European Union (European Regional Development Fund-ERDF corresponding to the multiannual financial framework 2014–2020), and the European Research Council (Advanced Grant No. 340055). S.G. thanks the European Union (European Regional Development Fund, Interreg V-A POCTEP España-Portugal programme, 2iqbioneuro project) and M.T.G. thanks the financial support from the Agencia Estatal de Investigación (RTI2018-093813-J-I00). The authors thank R. Menaya-Vargas for excellent technical assistance, the use of RIAIDT-USC analytical facilities and especially M. Marcos for excellent and essential contributions to the LC-MS analysis.

Conflict of Interest

The authors declare no conflict of interest.

Keywords: bioorthogonal chemistry · copper · intracellular chemistry · metal carbenes · metal catalysis

[1] a) S. Martínez Cuesta, S. A. Rahman, N. Furnham, J. M. Thornton, *Biophys. J.* **2015**, *109*, 1082 – 1086; b) B. Alberts, A. Johnson, J. Lewis, M. Raff, K. Roberts, P. Walter, *Molecular Biology of the Cell*, 6th ed., Garland Science, New York & Abingdon, **2017**.

[2] a) T. Vornholt, F. Christoffel, M. M. Pellizzoni, S. Panke, T. R. Ward, M. Jeschek, *Sci. Adv.* **2021**, *7*, eabe4208; b) J.-E. Bäckvall, M. Diéguez, O. Pamiès, *Artificial Metalloenzymes and MetalloDNAzymes in Catalysis: From Design to Applications*, Wiley-VCH, Weinheim, **2018**; c) F. Schwizer, Y. Okamoto, T. Heinisch, Y. Gu, M. M. Pellizzoni, V. Lebrun, R. Reuter, V. Köhler, J. C. Lewis, T. R. Ward, *Chem. Rev.* **2018**, *118*, 142 – 231; d) H. J. Davis, T. R. Ward, *ACS Cent. Sci.* **2019**, *5*, 1120 – 1136; e) T. Matsuo, T. Miyake, S. Hirota, *Tetrahedron Lett.* **2019**, *60*, 151226 – 151233; f) T. K. Hyster, T. R. Ward, *Angew. Chem. Int. Ed.* **2016**, *55*, 7344 – 7357; *Angew. Chem.* **2016**, *128*, 7468 – 7482; g) A. D. Liang, J. Serrano-Plana, R. L. Peterson, T. R. Ward, *Acc. Chem. Res.* **2019**, *52*, 585 – 595.

[3] a) D. Chordia, S. Narasimhan, A. L. Paioni, M. Baldus, G. Roelfes, *Angew. Chem. Int. Ed.* **2021**, *60*, 5913 – 5920; *Angew. Chem.* **2021**, *133*, 5978 – 5985; b) R.-V. Maaskant, S. Chordia, G. Roelfes, *ChemCatChem* **2021**, *13*, 1607 – 1613; c) M. Jeschek, S. Panke, T. R. Ward, *Trends Biotechnol.* **2018**, *36*, 60 – 72; d) K. Tanaka, K. Vong, *Proc. Jpn. Acad. Ser. B* **2020**, *96*, 79 – 94.

[4] a) P. Destito, C. Vidal, F. López, J. L. Mascareñas, *Chem. Eur. J.* **2021**, *27*, 4789 – 4816; b) Y. Liu, Y. Bai, *ACS Appl. Bio Mater.* **2020**, *3*, 4717 – 4746; c) M. Martínez-Calvo, J. L. Mascareñas, *Coord. Chem. Rev.* **2018**, *359*, 57 – 79; d) A. H. Ngo, S. Bose, L. H. Do, *Chem. Eur. J.* **2018**, *24*, 10584 – 10594; e) Y. Bai, J. Chen, S. C. Zimmerman, *Chem. Soc. Rev.* **2018**, *47*, 1811 – 1821; f) J. J. Soldevilla-Barreda, N. Metzler-Nolte, *Chem. Rev.* **2019**, *119*, 829 – 869; g) D. P. Nguyen, H. T. H. Nguyen, L. H. Do, *ACS Catal.* **2021**, *11*, 5148 – 5165.

[5] a) C. Streu, E. Meggers, *Angew. Chem. Int. Ed.* **2006**, *45*, 5645 – 5648; *Angew. Chem.* **2006**, *118*, 5773 – 5776; b) T. Völker, F. Dempwolff, P. L. Graumann, E. Meggers, *Angew. Chem. Int. Ed.* **2014**, *53*, 10536 – 10540; *Angew. Chem.* **2014**, *126*, 10705 – 10710; c) M. I. Sánchez, C. Penas, M. E. Vázquez, J. L. Mascareñas, *Chem. Sci.* **2014**, *5*, 1901 – 1907; d) G. Y. Tonga, Y. Jeong, B. Duncan, T. Mizuhara, R. Mout, R. Das, S. T. Kim, Y.-C. Yeh, B. Yan, S. Hou, V. M. Rotello, *Nat. Chem.* **2015**, *7*, 597 – 603; e) M. Tomás-Gamasa, M. Martínez-Calvo, J. R. Couceiro, J. L. Mascareñas, *Nat. Commun.* **2016**, *7*, 12538 – 12547; f) M. Martínez-Calvo, J. R. Couceiro, P. Destito, J. Rodríguez, J. Mosquera, J. L. Mascareñas, *ACS Catal.* **2018**, *8*, 6055 – 6061; g) B. J. Stenton, B. L. Oliveira, M. J. Matos, L. Sinatra, G. J. L. Bernardes, *Chem. Sci.* **2018**, *9*, 4185 – 4189; h) R. Martínez, C. Carrillo-Carrión, P. Destito, A. Álvarez, M. Tomás-Gamasa, B. Pelaz, F. López, J. L. Mascareñas, P. del Pino, *Cell. Rep. Phys. Sci.* **2020**, *1*, 100076.

[6] a) C. Vidal, M. Tomás-Gamasa, P. Destito, F. López, J. L. Mascareñas, *Nat. Commun.* **2018**, *9*, 1913; b) M. A. Miller, B. Askevold, H. Mikula, R. H. Kohler, D. Pirovich, R. Weissleder, *Nat. Commun.* **2017**, *8*, 15906 – 15918.

[7] a) P. Destito, A. Sousa-Castillo, J. R. Couceiro, F. López, M. A. Correa-Duarte, J. L. Mascareñas, *Chem. Sci.* **2019**, *10*, 2598 – 2603; b) R. M. Yusop, A. Unciti-Broceta, E. M. V. Johansson, R. M. Sánchez-Martín, M. Bradley, *Nat. Chem.* **2011**, *3*, 239 – 243; c) S. N. W. Toussaint, R. T. Calkins, S. Lee, B. W. Michel, *J. Am. Chem. Soc.* **2018**, *140*, 13151 – 13155; d) F. Wang, Y. Zhang, Z. Du, J. Ren, X. Qu, *Nat. Commun.* **2018**, *9*, 1209.

[8] a) P. Destito, J. R. Couceiro, H. Ferreira, F. López, J. L. Mascareñas, *Angew. Chem. Int. Ed.* **2017**, *56*, 10766 – 10770; *Angew. Chem.* **2017**, *129*, 10906 – 10910; b) J. Miguel-Ávila, M. Tomás-Gamasa, J. L. Mascareñas, *Angew. Chem. Int. Ed.* **2020**, *59*, 17628 – 17633; *Angew. Chem.* **2020**, *132*, 17781 – 17786; c) J. Miguel-Ávila, M. Tomás-Gamasa, A. Olmos, P. J. Pérez, J. L. Mascareñas, *Chem. Sci.* **2018**, *9*, 1947 – 1952; d) S. Li, L. Wang, F. Yum, Z. Zhu, D. Shobaki, H. Chen, M. Wang, J. Wang, G. Qin, U. J. Erasquin, L. Ren, Y. Wang, C. Cai, *Chem. Sci.* **2017**, *8*, 2107 – 2114; e) Y. Bai, X. Feng, H. Xing, Y. Xu, B. K. Kim, N. Baig, T. Zhou, A. A. Gewirth, Y. Lu, E. Oldfield, S. C. Zimmerman, *J. Am. Chem. Soc.* **2016**, *138*, 11077 – 10080.

[9] F. Zaragoza Dörwald, *Metal Carbenes in Organic Synthesis*, Wiley-VCH, Weinheim, **1999**.

[10] a) K. A. Mix, M. R. Aronoff, R. T. Raines, *ACS Chem. Biol.* **2016**, *11*, 3233 – 3244; b) K. A. Andersen, M. R. Aronoff, N. A. McGrath, R. T. Raines, *J. Am. Chem. Soc.* **2015**, *137*, 2412 – 2415; c) S.-Y. Dai, D. A. Yang, *J. Am. Chem. Soc.* **2020**, *142*, 17156 – 17166; d) J. M. Antos, M. B. Francis, *J. Am. Chem. Soc.* **2004**, *126*, 10256 – 10257; e) J. M. Antos, J. M. McFarland, A. T. Lavarone, M. B. Francis, *J. Am. Chem. Soc.* **2009**, *131*, 6301 – 6308.

[11] a) B. V. Popp, Z. T. Ball, *J. Am. Chem. Soc.* **2010**, *132*, 6660 – 6662; b) B. V. Popp, Z. T. Ball, *Chem. Sci.* **2011**, *2*, 690 – 695; c) Z. Chen, F. Vohidov, J. M. Coughlin, L. J. Stagg, S. T. Arold, J. E.

Ladbury, Z. T. Ball, *J. Am. Chem. Soc.* **2012**, *134*, 10138 – 10145; d) F. Vohidov, J. M. Coughlin, Z. T. Ball, *Angew. Chem. Int. Ed.* **2015**, *54*, 4587 – 4591; *Angew. Chem.* **2015**, *127*, 4670 – 4674; e) J. Ohata, Z. T. Ball, *J. Am. Chem. Soc.* **2017**, *139*, 12617 – 12622.

[12] a) K. Tishinov, K. Schmidt, D. Häussinger, D. G. Gillingham, *Angew. Chem. Int. Ed.* **2012**, *51*, 12000 – 12004; *Angew. Chem.* **2012**, *124*, 12166 – 12170; b) K. Tishinov, N. Fei, D. Gillingham, *Chem. Sci.* **2013**, *4*, 4401 – 4406.

[13] a) H. M. Key, P. Dydio, D. S. Clark, J. F. Hartwig, *Nature* **2016**, *534*, 534 – 537; b) P. Dydio, H. M. Key, A. Nazarenko, J. Y.-E. Rha, V. Seyedkazemi, D. S. Clark, J. F. Hartwing, *Science* **2016**, *354*, 102 – 106; c) R. K. Zhang, K. Chen, X. Huang, L. Wohlschlager, H. Renata, F. H. Arnold, *Nature* **2019**, *565*, 67 – 72; d) P. S. Coelho, Z. J. Wang, M. E. Ener, S. A. Baril, A. Kannan, F. H. Arnold, E. M. Brustad, *Nat. Chem. Biol.* **2013**, *9*, 485 – 487; e) S. B. J. Kan, R. D. Lewis, K. Chen, F. H. Arnold, *Science* **2016**, *354*, 1048 – 1051; f) R. D. Lewis, M. García-Borrás, M. J. Chalkley, A. R. Buller, K. N. Houk, S. B. J. Kan, F. H. Arnold, *Proc. Natl. Acad. Sci. USA* **2018**, *115*, 7308 – 7313; g) S. B. J. Kan, X. Huang, Y. Gumulya, K. Chen, F. H. Arnold, *Nature* **2017**, *552*, 132 – 136; h) A. L. Chandgude, X. Ren, R. Fasan, *J. Am. Chem. Soc.* **2019**, *141*, 9145 – 9150; i) G. Sreenilayam, R. Fasan, *Chem. Commun.* **2015**, *51*, 1532 – 1534.

[14] a) F. H. Arnold, *Angew. Chem. Int. Ed.* **2018**, *57*, 4143 – 4148; *Angew. Chem.* **2018**, *130*, 4212 – 4218; b) S. Wallace, E. P. Balskus, *Angew. Chem. Int. Ed.* **2015**, *54*, 7106 – 7109; *Angew. Chem.* **2015**, *127*, 7212 – 7215; c) S. Wallace, E. P. Balskus, *Angew. Chem. Int. Ed.* **2016**, *55*, 6023; *Angew. Chem.* **2016**, *128*, 6127.

[15] R. M. Pandit, S. H. Kim, Y. R. Lee, *Adv. Synth. Catal.* **2016**, *358*, 3586 – 3599.

[16] a) C. Uttamapinant, A. Tangpeerachaikul, S. Grecian, S. Clarke, U. Singh, P. Slade, K. R. Gee, A. Y. Ting, *Angew. Chem. Int. Ed.* **2012**, *51*, 5852 – 5856; *Angew. Chem.* **2012**, *124*, 5954 – 5958; b) V. Bevilacqua, M. King, M. Chaumontet, M. Nothisen, S. Gabillet, D. Buisson, C. Puente, A. Wagner, F. Taran, *Angew. Chem. Int. Ed.* **2014**, *53*, 5872 – 5876; *Angew. Chem.* **2014**, *126*, 5982 – 5986; c) S. N. Geigle, L. A. Wyss, S. J. Sturla, D. G. Gillingham, *Chem. Sci.* **2017**, *8*, 499 – 506.

[17] K. Ramakrishna, C. Sivasankar, *Org. Biomol. Chem.* **2017**, *15*, 2392 – 2396.

[18] T. Kitanosono, S. Kobayashi, *ACS Cent. Sci.* **2021**, *7*, 739 – 747.

[19] a) E. M. Sletten, C. R. Bertozzi, *Angew. Chem. Int. Ed.* **2009**, *48*, 6974 – 6998; *Angew. Chem.* **2009**, *121*, 7108 – 7133; b) S. Shaligram, A. Campbell, *Toxicol. In Vitro* **2013**, *27*, 844 – 851.

[20] M. O. N. van de L'Isle, M. C. Ortega-Liebana, A. Unciti-Broceta, *Curr. Opin. Chem. Biol.* **2021**, *61*, 32 – 42.

[21] a) C. Vidal, M. Tomás-Gamasa, A. Gutiérrez-González, J. L. Mascareñas, *J. Am. Chem. Soc.* **2019**, *141*, 5125 – 5129; b) V. Sabatino, J. G. Rebelein, T. R. Ward, *J. Am. Chem. Soc.* **2019**, *141*, 17048 – 17052; c) J. S. Huang, L. Wang, P. Zhao, F. Xiang, J. Liu, S. Zhang, *ACS Catal.* **2018**, *8*, 5941 – 5946; d) F. Wang, Y. Zhang, Z. Liu, Z. Du, L. Zhang, J. Ren, X. A. Qu, *Angew. Chem. Int. Ed.* **2019**, *58*, 6987 – 6992; *Angew. Chem.* **2019**, *131*, 7061 – 7066; e) A. Sousa-Castillo, J. R. Couceiro, M. Tomás-Gamasa, A. Mariño-López, F. López, W. Baaziz, O. Ersen, M. Comesaña-Hermo, J. L. Mascareñas, M. A. Correa-Duarte, *Nano Lett.* **2020**, *20*, 7068 – 7076.

[22] a) A. Levitzki, E. Mishani, *Annu. Rev. Biochem.* **2006**, *75*, 93 – 109; b) S. J. Park, Y. J. Park, J. H. Shin, E. S. Kim, J. J. Hwang, D. H. Jin, J. C. Kim, D.-H. Cho, *Biochem. Biophys. Res. Commun.* **2011**, *408*, 465 – 470.

[23] A. Gazit, H. App, G. McMahon, A. Chen, A. Levitzki, F. D. Bohmer, *J. Med. Chem.* **1996**, *39*, 2170.

[24] A. Gazit, K. Yee, A. Uecker, F. D. Böhmer, T. Sjöblom, A. Ostman, J. Waltenberger, G. Golomb, S. Banai, M. C. Heinrich, A. Levitzki, *Bioorg. Med. Chem.* **2003**, *11*, 2007 – 2018.

[25] S. Chalmers, S. T. Caldwell, C. Quin, T. A. Prime, A. M. James, A. G. Cairns, M. P. Murphy, J. G. McCarron, R. C. Hartley, *J. Am. Chem. Soc.* **2012**, *134*, 758 – 761.

[26] S. Learte-Aymamí, C. Vidal, A. Gutiérrez-González, J. L. Mascareñas, *Angew. Chem. Int. Ed.* **2020**, *59*, 9149 – 9154; *Angew. Chem.* **2020**, *132*, 9234 – 9239.

Manuscript received: July 5, 2021
Accepted manuscript online: August 13, 2021
Version of record online: August 26, 2021

